HHS Public Access

Author manuscript

Angew Chem Int Ed Engl. Author manuscript; available in PMC 2016 November 23.

Published in final edited form as:

Angew Chem Int Ed Engl. 2015 November 23; 54(48): 14398–14401. doi:10.1002/anie.201507227.

A Eu(II)-Containing Cryptate as a Redox Sensor in Magnetic Resonance Imaging of Living Tissue**

Levi A. Ekanger,
Department of Chemistry, Wayne State University, 5101 Cass Avenue, Detroit, MI 48202, USA

Lisa A. Polin,
Department of Oncology, Wayne State University School of Medicine, 110 East Warren Avenue, Detroit, MI 48201, USA

Barbara Ann Karmanos Cancer Institute, 4100 John R. Street, Detroit, MI 48201, USA

Yimin Shen,
Department of Radiology, Wayne State University School of Medicine, 3990 John R. Street, Detroit, MI 48201, USA

E. Mark Haacke,
Department of Radiology, Wayne State University School of Medicine, 3990 John R. Street, Detroit, MI 48201, USA

Barbara Ann Karmanos Cancer Institute, 4100 John R. Street, Detroit, MI 48201, USA

Philip D. Martin, and
Lumigen Instrument Center, Chemistry Department, Wayne State University, 5101 Cass Avenue, Detroit, MI 48202, USA

Matthew J. Allen*
Department of Chemistry, Wayne State University, 5101 Cass Avenue, Detroit, MI 48202, USA

Barbara Ann Karmanos Cancer Institute, 4100 John R. Street, Detroit, MI 48201, USA

Abstract

Eu^{II} rivals Gd^{III} in its ability to enhance contrast in magnetic resonance imaging; however, all reported Eu^{II}-based complexes have been studied in vitro largely because the tendency of Eu^{II} to oxidize to Eu^{III} has been viewed as a major obstacle to in vivo imaging. Here, we present solid- and solution-phase characterization of a Eu^{II}-containing cryptate and first in vivo use of Eu^{II} to provide contrast enhancement. The results are indicative of a water-coordination number between one and two upon dissolution and are a demonstration of the ability to observe Eu^{II}-based contrast enhancement for hours in a mouse.

**The authors acknowledge the National Institutes of Health (NIH) for support (R01EB013663). The Biobanking and Correlative Sciences Core and the Animal Model and Therapeutics Evaluation Core are supported, in part, by an NIH Center grant (P30CA022453) to the Barbara Ann Karmanos Cancer Institute at Wayne State University (WSU). The authors are grateful to WSU for a Thomas C. Rumble Graduate Research Fellowship (L. A. E.) and a Schaap Faculty Scholar Award (M. J. A.).

*M. J. Allen: mallen@chem.wayne.edu, Homepage: http://chem.wayne.edu/allengroup.

Supporting information for this article is given via a link at the end of the document.

Keywords

cryptands; divalent; europium; imaging agents; in vivo

Magnetic resonance imaging (MRI) is a powerful diagnostic tool for imaging opaque tissues at relatively high spatial resolution and nearly unlimited depth penetration.[1] Paramagnetic complexes are routinely used as contrast agents in clinical MRI to provide contrast enhancement in areas of anatomical interest. For decades, Gd^{III} has been the paramagnetic metal ion of choice for contrast agents largely because it has seven unpaired electrons (S = 7/2) in an isotropic ground state configuration ($^8S_{7/2}$). Eu^{II} is isoelectronic with Gd^{III}, and both ions enhance contrast in MRI.[2] Furthermore, Eu^{II} has a propensity to oxidize to Eu^{III}, resulting in a diamagnetic ground state ($^7F_0$) and thermally accessible excited state ($^7F_1$) that do not noticeably enhance contrast in MRI.[3] Therefore, the oxidation of Eu^{II} offers the opportunity for metal-based redox-responsive contrast enhancement that is unachievable with Gd^{III}-based contrast agents. However, despite several groups exploring Eu^{II}-based complexes as contrast agents for MRI,[2–4] there has been no reported use of Eu^{II} in vivo. Here, we report the first in vivo use of a Eu^{II}-containing cryptate. We also report characterization that reveals a discrepancy in coordination environment between solid- and solution-phase.

We chose to characterize and attempt in vivo imaging with Eu^{II}-222Fb (222Fb = 5,6-(4-fluorobenzo)-4,7,13,16,21,24-hexaoxa-1,10-diazabicyclo[8.8.8]hexacos-5-ene, Figure 1) because it has a relatively positive oxidation peak potential (0.366 V vs normal hydrogen electrode).[4f] More positive potentials favor the +2 oxidation state that is desirable for imaging. However, Eu^{II}-222Fb is prone to oxidation by molecular oxygen, and the Eu^{II} ion in this cryptate was expected to be oxidized to Eu^{III} in tissues containing appreciable levels of molecular oxygen or other strong oxidants. In healthy tissue, intracellular environments tend to be reducing while extracellular environments tend to be oxidizing, but in necrotic tissue, dead cells leach components of the cytosol into extracellular space to create a relatively reducing environment.[5] We hypothesized that the reducing environment of necrotic tissue would prevent oxidation of Eu^{II}-222Fb and, consequently, contrast enhancement would be observed in necrotic tissue in the presence of Eu^{II}-222Fb. Before imaging in vivo, we characterized Eu^{II}-222Fb using solid- and solution-phase techniques.

The X-ray crystal structure of Eu^{II}-222Fb (Figure 1b) features a nine-coordinate metal center in an eclipsed hula-hoop geometry.[6] Eight coordination sites are occupied by six oxygen and two nitrogen atoms of 222Fb and the ninth site is occupied by a coordinated chloride counteranion. Interestingly, this nine-coordinate geometry is different than the ten-coordinate geometry of a Sr^{II}-containing [2.2.2] cryptate (without the fluorobenzo group) that contains a coordinated water molecule and coordinated trifluoromethanesulfonate anion.[4h] This difference is noteworthy because Sr^{II} and Eu^{II} have similar ionic radii, and Sr^{II} is often used as a diamagnetic analog for Eu^{II}. Because coordination environment is a key parameter in the characterization of contrast agents for MRI, we interrogated the coordination environment of Eu^{II}-222Fb in solution.

To test whether chloride remained coordinated in solution, we measured the molar conductivity of Eu^{II}-222Fb in water. The molar conductivity was 211 ± 1 S cm^2 mol^{-1}, which is consistent with compounds exhibiting a 2:1 dissociation in water.[7] This observation indicates that, on average, no chlorides are coordinated to Eu^{II} in solution. However, because molar conductivity is a colligative property, it does not provide further information regarding the coordination environment of Eu^{II}-222Fb in solution.

To further characterize the coordination environment of Eu^{II}-222Fb in solution, we used variable-temperature ^{17}O-NMR spectroscopy to investigate water coordination. Using 1% enriched $H_2{}^{17}O$ in phosphate-buffered saline, we were able to observe a paramagnetic broadening of the ^{17}O-NMR signal upon addition of Eu^{II}-222Fb. The line broadening is consistent with the presence of inner sphere water. This observation coupled with a 2:1 dissociation suggests that in solution Eu^{II}-222Fb is present either as a nine-coordinate species with chloride displaced by a water molecule or as a ten-coordinate species, based on the ability of Eu^{II} to adopt ten-coordinate geometries,[8] with two coordinated water molecules after chloride dissociation (Figure 2b). It is unlikely that more than two water molecules coordinate because 222Fb occupies eight coordination sites and because to the best of our knowledge, no eleven-coordinate molecular Eu^{II}-containing complexes have been reported. After studying the coordination environment of Eu^{II}-222Fb, we turned to in vitro MRI to characterize its ability to influence contrast.

To characterize the ability of Eu^{II}-222Fb to provide contrast enhancement, we measured the relaxivity of Eu^{II}-222Fb in phosphate-buffered saline using T_1-weighted MRI. The relaxivity (24 °C, 7 T) of Eu^{II}-222Fb in phosphate-buffered saline was 6.5 ± 0.3 mM^{-1} s^{-1}. Our measured relaxivity in phosphate-buffered saline is in agreement with other Eu^{II}-containing cryptates.[2b] Additionally, phosphate can bind lanthanide ions in a bidentate manner to displace two water molecules when the metal ion contains two adjacent coordinated water molecules.[9] Nonadjacent water would be consistent with water molecules replacing the two chloride ions (Figure 2b). While not coordinated, the outer sphere chloride is 5.383 Å from Eu^{II} (the coordinated chloride is 2.793 Å from Eu^{II}), and if both chloride ions are replaced by water molecules, a closer approach could be envisioned due to the smaller size of oxygen relative to chloride. Accordingly, our measured ^{17}O line broadening, crystal structure, and relaxivity suggest that if two water molecules are coordinated to Eu^{II}-222Fb in solution, that they are likely not adjacent to each other.

To test whether Eu^{II}-222Fb would enhance contrast in necrotic tissue, we performed T_1-weighted MRI before and after intratumoral injection of Eu^{II}-222Fb (50 μL, 19.4 mM) into a 4T1 mammary carcinoma. The 4T1 carcinoma model is an aggressive tumor that typically develops a necrotic core,[10] and imaging was performed when tumors reached approximately 700–1000 mg to maximize the probability of necrosis. Images were acquired before and at 3, 20, and 120 min after intratumoral injection (Figure 3a–d). Positive contrast enhancement was observed for the entirety of the 120 min experiment, but the location of positive contrast enhancement changed over time. Specifically, heterogeneous positive contrast enhancement was observed along nearly the entire length of the tumor immediately post injection, but was only observed in a localized core of the tumor after 120 min. These observations demonstrate that Eu^{II} persists within a tumor for at least 120 min, and we

observed this duration of positive contrast enhancement in all seven of our attempted imaging experiments with independently injected tumors. The presence of contrast enhancement is consistent with the persistence of the +2 oxidation state of europium in the core of the tumor, and the reduced oxidation state is suggestive of a lack of oxygen.

To verify the presence of necrotic tissue in the tumor, we sacrificed the mouse directly after the 120 min post-injection image and performed histological staining. The tumor was removed in whole, fixed in formalin, mounted in paraffin, and cut to a thickness of 5 μm before being stained with hematoxylin and eosin (Figure 3f). Hematoxylin is a dye that stains nuclei, and eosin stains elements of the cytoplasm as a counterstain to differentiate areas that are nuclei-abundant (blue) from those that are nuclei-deficient (pink).[11] Areas associated with necrosis are expected to stain pink to a greater extent than non-necrotic areas because of the lack of cells and their corresponding nuclei in necrotic regions. The stained slice revealed nuclei-deficient regions consistent with necrosis that were particularly pronounced in the mid-to-upper half of the tumor. The leftmost region of the slice stained pink from the presence of tumor ulceration through the mouse epidermis. Consistent with staining, the majority of positive contrast enhancement observed 120 min post-injection was in the mid-to-upper half of the tumor, suggesting that Eu^{II}-222Fb provided positive contrast enhancement in the necrotic core of the tumor (Figure 3g). No contrast enhancement was observed in the leftmost region of the tumor likely because of direct contact between tumor ulceration and oxygen in the air. It is worth reiterating that we used an intratumoral injection, which may have placed a bolus in the tumor core and the lack of oxygen allowed Eu^{II} to persist.

To better understand the potential mechanism of differentiation, we performed an intratumoral injection of Eu^{II}-222Fb (50 μL, 6.9 mM) and monitored contrast enhancement over the course of 3 h before sacrificing the mouse and removing the injected tumor for analysis of Eu content by inductively coupled plasma mass spectrometry. At 3 h post-injection, we observed a decrease in positive contrast enhancement (~85%) in the tumor relative to the initial image and a decrease of in the Eu content (~80%) in the tumor relative to the injected dose. These close values suggest clearance of Eu^{II}-222Fb played a major role in the loss of positive contrast enhancement. Clearance was not directly observed in T_1-weighted MRI because Eu^{II}-222Fb likely oxidized in tissues or fluids of relatively higher oxygen content, and the product of oxidation, Eu^{III}, does not produce positive contrast enhancement. Furthermore, when Gd^{III}-1,4,7,10-tetraazacyclododecane-1,4,7,10-tetraacetate (50 μL, 20.5 mM) was injected into a tumor in a separate experiment, the bladder of the mouse was bright with contrast within minutes of the injection. We observed this phenomenon in two independently injected tumors. This non-redox-active control indicates that the concentration of Eu^{II} injected should be enough to visualize in the bladder if clearance occurred without oxidation. The evidence of clearance based on Eu content and the lack of contrast enhancement observed outside of the tumor demonstrates the lack of background enhancement possible with Eu^{II}-based imaging agents in redox-active environments. While the connection between positive contrast enhancement and necrotic tissue is intriguing, more detailed experiments are required to evaluate the nature of

Eu^{II}-222Fb clearance over time. Regardless of the mechanism of differentiation, our in vivo imaging data demonstrate the first reported use Eu^{II} for in vivo contrast-enhanced MRI.

To investigate the in vitro stability of Eu^{II}-222Fb with respect to oxygen exposure, we measured T_1 (37 °C, 1.4 T) of Eu^{II}-222Fb in phosphate-buffered saline to monitor the oxidation of Eu^{II} as a function of air exposure while stirring. Under an atmosphere of N_2 ($pO_2 \approx 0$ mmHg), Eu^{II}-222Fb remained in the +2 oxidation for at least 118 d. However, upon stirring in open air ($pO_2 \approx 160$ mmHg), the observed T_1 enhancement was completely lost within 5 min. This rapid oxidation with elevated oxygen exposure suggests that Eu^{II}-222Fb is oxidized upon clearance from the oxygen-deficient 4T1 necrotic core ($pO_2 \leq 10$ mmHg)[12,13] into relatively oxygenated vasculature ($pO_2 \approx 40$–100 mmHg).[14] Collectively, the persistence of the +2 oxidation state over a 120 min period, the correlation between necrotic tissue and contrast enhancement, the lack of positive contrast enhancement in organs associated with clearance (bladder, liver, or kidneys), and the rapid oxidation observed in elevated air exposure suggest that Eu^{II}-222Fb persists in the poorly oxygenated necrotic core of the tumors and oxidizes elsewhere.

In conclusion, we report solid- and solution-phase characterization of Eu^{II}-222Fb that is nine-coordinate in the solid state and nine- or ten-coordinate in solution. Additionally, we report the first in vivo contrast-enhanced MRI with a Eu^{II}-based contrast agent, and efforts in our laboratory to understand the behavior of Eu^{II}-222Fb in vivo are underway. We expect that the ability to differentiate necrotic from non-necrotic tissue in vivo coupled with the tunable oxidation potential of Eu^{II} will enable bracketing of tissue redox environments associated with both hypoxic and hyperoxic tissues relevant to the study of many diseases.

Supplementary Material

Refer to Web version on PubMed Central for supplementary material.

References

1. a) Radecki G, Nargeot R, Jelescu IO, Le Bihan D, Ciobanu L. Proc Natl Acad Sci USA. 2014; 111:8667–8672. [PubMed: 24872449] b) van Veluw SJ, Zwanenburg JJM, Engelen-Lee J, Spliet WGM, Hendrikse J, Luijten PR, Biessels GJ. J Cereb Blood Flow Metab. 2013; 33:322–329. [PubMed: 23250109]
2. a) Ekanger LA, Allen MJ. Metallomics. 2015; 7:405–421. [PubMed: 25579206] b) Garcia J, Neelavalli J, Haacke EM, Allen MJ. Chem Commun. 2011; 47:12858–12860.
3. Ekanger LA, Ali MM, Allen MJ. Chem Commun. 2014; 50:14835–14838.
4. a) Regueiro-Figueroa M, Barriada JL, Pallier A, Esteban-Gómez D, de Blas A, Rodríguez-Blas T, Tóth É, Platas-Iglesias C. Inorg Chem. 2015; 54:4940–4952. [PubMed: 25942280] b) Kuda-Wedagedara ANW, Wang C, Martin PD, Allen MJ. J Am Chem Soc. 2015; 137:4960–4963. [PubMed: 25853298] c) Gál M, Kielar F, Sokolová R, Ramešová Š, Kolivoška V. Eur J Inorg Chem. 2013; 2013:3217–3223.d) Garcia J, Allen MJ. Inorg Chim Acta. 2012; 393:324–327.e) Garcia J, Kuda-Wedagedara ANW, Allen MJ. Eur J Inorg Chem. 2012; 2012:2135–2140. [PubMed: 22639543] f) Gamage NDH, Mei Y, Garcia J, Allen MJ. Angew Chem Int Ed. 2010; 49:8923–8925. *Angew. Chem.***2010**, *122*, 9107–9109. g) Burai L, Tóth É, Moreau G, Sour A, Scopelliti R, Merbach AE. Chem Eur J. 2003; 9:1394–1404. [PubMed: 12645029] h) Burai L, Scopelliti R, Tóth É. Chem Commun. 2002:2366–2367.i) Caravan P, Tóth É, Rockenbauer A, Merbach AE. J Am Chem Soc. 1999; 121:10403–10409.

5. a) Lotze MT, Zeh HJ, Rubartelli A, Sparvero LJ, Amoscato AA, Washburn NR, DeVera ME, Liang X, Tör M, Billiar T. Immunol Rev. 2007; 220:60–81. [PubMed: 17979840] b) Rubartelli A, Lotze MT. Trends Immunol. 2007; 28:429–436. [PubMed: 17845865]
6. Ruiz-Martínez A, Casanova D, Alvarez S. Chem Eur J. 2008; 14:1291–1303. [PubMed: 18000919]
7. Apelblat A, Esteso MA, Bešter-Rogač M. J Phys Chem B. 2013; 117:5241–5248. [PubMed: 23534843]
8. Christoffers J, Starynowicz P. Polyhedron. 2008; 27:2688–2692.
9. Supkowski RM, Horrocks WD. Inorg Chem. 1999; 38:5616–5619. [PubMed: 11671291]
10. Tao K, Fang M, Alroy J, Sahagian GG. BMC Cancer. 2008; 8:228. [PubMed: 18691423]
11. Degenhardt K, Mathew R, Beaudoin B, Bray K, Anderson D, Chen G, Mukherjee C, Shi Y, Gélinas C, Fan Y, Nelson DA, Jin S, White E. Cancer Cell. 2006; 10:51–64. [PubMed: 16843265]
12. Hardee ME, Dewhirst MW, Agarwal N, Sorg BS. Curr Mol Med. 2009; 9:435–441. [PubMed: 19519401]
13. Leow MKS. Adv Physiol Educ. 2007; 31:198–201. [PubMed: 17562911]
14. Carreau A, Hafny-Rahbi BE, Matejuk A, Grillon C, Kieda C. J Cell Mol Med. 2011; 15:1239–1253. [PubMed: 21251211]

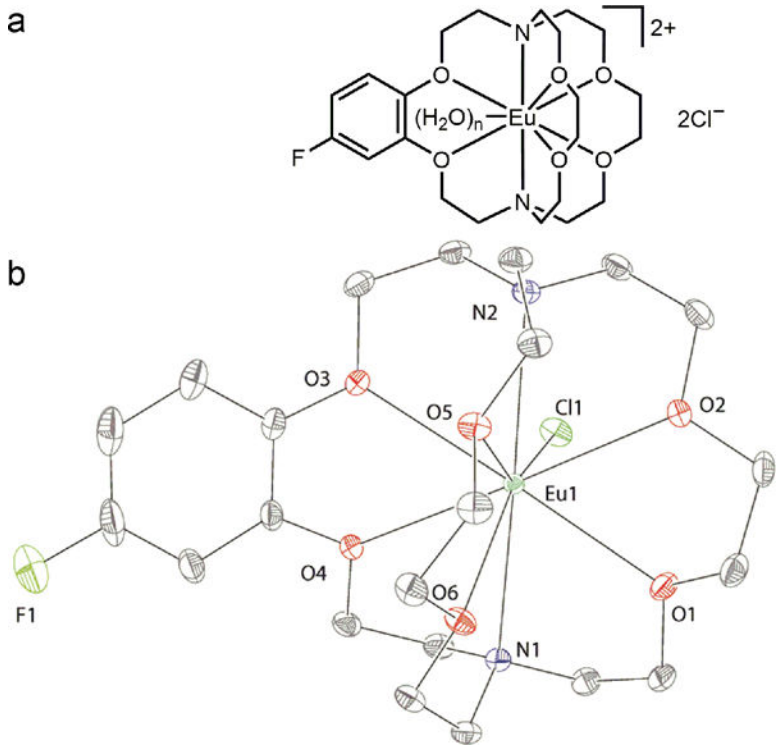

Figure 1.

(a) Proposed solution-phase structure of Eu^{II}-222Fb with non-coordinated chloride counteranions and one or two coordinated water molecules (n = 1 or 2). (b) X-ray crystal structure of Eu^{II}-222Fb with a coordinated chloride ion (hydrogen atoms and the outer sphere chloride counteranion are not shown for clarity). *R*-factor = 0.0248. Resolution = 0.59 Å. Thermal ellipsoids are drawn at the 50% probability level.

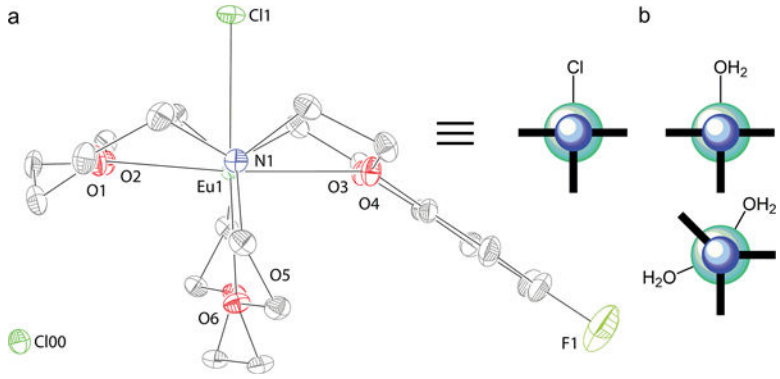

Figure 2.

(a) X-ray crystal structure (viewed along the N–Eu–N axis) of Eu^{II}-222Fb (hydrogen atoms are not shown for clarity) alongside a cartoon representation of the solid-phase geometry in the same orientation as the crystal structure. Outer sphere chloride, Cl00, related by symmetry is included in the image. (b) Cartoon representation of the proposed solution-phase geometry of Eu^{II}-222Fb with one or two coordinated water molecules viewed along the N–Eu–N axis. The blue and teal spheres in the cartoons represent nitrogen and europium, respectively, and the bold lines represent the cryptands. *R*-factor = 0.0248. Resolution = 0.59 Å. Thermal ellipsoids are drawn at the 50% probability level.

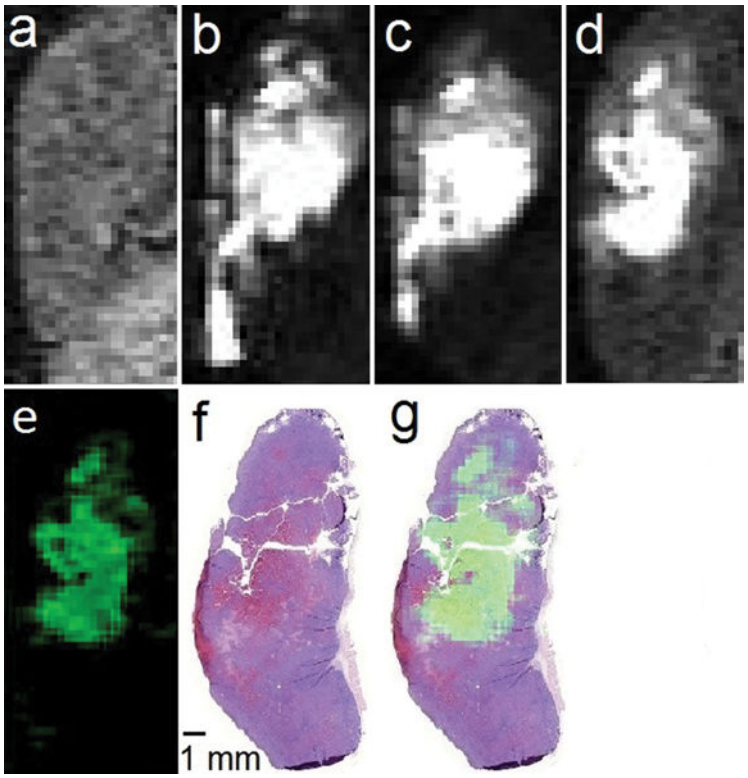

Figure 3.

T_1-weighted in vivo sagittal plane images of a 4T1 tumor injected with Eu^{II}-222Fb (a) pre-injection; (b) 3 min, (c) 20 min, and (d) 120 min post-intratumoral injection; (e) difference between the 120 min and pre-injection images (image d minus image a) colored using the ImageJ green lookup table; (f) hematoxylin- and eosin-stained slice of tumor imaged in a–e; and (g) sum of images e and f. All images are on the same scale. Imaging parameters included an echo time of 1.5 ms, repetition time of 11 ms, flip angle of 40°, field of view of 30 mm × 90 mm, and an in-plane resolution of 0.352 mm × 0.352 mm.